

Kent Academic Repository

Full text document (pdf)

Citation for published version

Schneider, Constanze and Oellerich, Thomas and Baldauf, Hanna-Mari and Schwarz, Sarah-Marie and Thomas, Dominique and Flick, Robert and Bohnenberger, Hanibal and Kaderali, Lars and Stegmann, Lena and Cremer, Anjali and Martin, Margarethe and Lohmeyer, Julian and Michaelis, Martin and Hornung, Veit and Schliemann, Christoph and Berdel, Wolfgang E and Hartmann,

DOI

<https://doi.org/10.1038/nm.4255>

Link to record in KAR

<http://kar.kent.ac.uk/60380/>

Document Version

Author's Accepted Manuscript

Copyright & reuse

Content in the Kent Academic Repository is made available for research purposes. Unless otherwise stated all content is protected by copyright and in the absence of an open licence (eg Creative Commons), permissions for further reuse of content should be sought from the publisher, author or other copyright holder.

Versions of research

The version in the Kent Academic Repository may differ from the final published version.

Users are advised to check <http://kar.kent.ac.uk> for the status of the paper. **Users should always cite the published version of record.**

Enquiries

For any further enquiries regarding the licence status of this document, please contact:

researchsupport@kent.ac.uk

If you believe this document infringes copyright then please contact the KAR admin team with the take-down information provided at <http://kar.kent.ac.uk/contact.html>

1 **SAMHD1 is a biomarker for cytarabine response and a therapeutic target**
2 **in acute myeloid leukemia**

3 Constanze Schneider^{1,§}, Thomas Oellerich^{2,3,4, §}, Hanna-Mari Baldauf^{1,5§}, Sarah-Marie
4 Schwarz^{1,§}, Dominique Thomas⁶, Robert Flick⁷, Hanibal Bohnenberger⁸, Lars Kaderali⁹, Lena
5 Stegmann¹, Anjali Cremer³, Margarethe Martin¹, Julian Lohmeyer³, Martin Michaelis¹⁰, Veit
6 Hornung^{11,12}, Christoph Schliemann¹³, Wolfgang E. Berdel¹³, Wolfgang Hartmann¹⁴, Eva
7 Wardelmann¹⁴, Federico Comoglio³, Martin-Leo Hansmann¹⁵, Alexander F. Yakunin⁷, Gerd
8 Geisslinger^{6,16}, Philipp Ströbel⁸, Nerea Ferreirós⁶, Hubert Serve^{2,4,*}, Oliver T. Keppler^{1,5,**} &
9 Jindrich Cinatl Jr.^{1,**}

10

¹Institute of Medical Virology, University of Frankfurt, Frankfurt, Germany. ²Department of Medicine II, Hematology/Oncology, Goethe University of Frankfurt, Frankfurt, Germany.

³Cambridge University Department of Haematology, Cambridge Institute of Medical Research, Cambridge, United Kingdom. ⁴German Cancer Consortium/ German Cancer Research Center, Heidelberg, Germany. ⁵Max von Pettenkofer-Institute, Department of Virology, Ludwig Maximilian University of Munich, Munich, Germany. ⁶pharmazentrum frankfurt/ZAFES, Institute of Clinical Pharmacology, Goethe University of Frankfurt, Frankfurt, Germany. ⁷Department of Chemical Engineering and Applied Chemistry, University of Toronto, Toronto, Ontario, Canada. ⁸Institute of Pathology, University Medical Center, Göttingen, Germany. ⁹Institute of Bioinformatics, University Medicine Greifswald, Greifswald, Germany. ¹⁰Centre for Molecular Processing and School of Biosciences, University of Kent, Canterbury United Kingdom. ¹¹Institute of Molecular Medicine, University Hospital Bonn, Bonn, Germany. ¹²Gene Center and Department of Biochemistry, Ludwig Maximilian University of Munich, Munich, Germany. ¹³Department of Medicine A (Hematology, Oncology), University Hospital Münster, Germany. ¹⁴Gerhard Domagk Institute for Pathology, University Hospital Münster, Germany. ¹⁵Senckenberg Institute of Pathology, University of Frankfurt, Frankfurt, Germany. ¹⁶Fraunhofer Institute for Molecular Biology and Applied Ecology (IME), Project group Translational Medicine and Pharmacology (TMP), Frankfurt, Germany.

11

12 [§]C.S., T.O., H.-M.B. and S.-M.S. contributed equally

13 *Co-correspondence for clinical studies: H.S. (Hubert.Serve@kgu.de)

14 **Senior co-correspondence: O.T.K. (keppler@mvp.uni-muenchen.de) or J.C.

15 (Cinatl@em.uni-frankfurt.de)

16 The nucleoside analog cytarabine (Ara-C) is an essential component of primary and
17 salvage chemotherapy regimens in acute myeloid leukemia (AML). After cellular
18 uptake, Ara-C is converted into its therapeutically active triphosphate metabolite, Ara-
19 CTP, which exerts anti-leukemic effects primarily by inhibiting DNA synthesis in
20 proliferating cells¹. Currently, a substantial fraction of AML patients fails to effectively
21 respond to Ara-C therapy and reliable biomarkers are lacking^{2,3}. SAMHD1 is a
22 deoxynucleoside triphosphate (dNTP) triphosphohydrolase that cleaves physiological
23 dNTPs into deoxyribonucleosides and inorganic triphosphate^{4,5}. Although it has been
24 postulated that SAMHD1 sensitizes cancer cells to nucleoside analog derivatives through
25 depletion of competing dNTPs⁶, we show here that SAMHD1 reduces Ara-C cytotoxicity
26 in AML cells. Mechanistically, dGTP-activated SAMHD1 hydrolyzes Ara-CTP,
27 resulting in a drastic reduction of Ara-CTP in leukemic cells. Loss of SAMHD1 activity -
28 through genetic depletion, mutational inactivation of its triphosphohydrolase activity, or
29 proteasomal degradation using specialized virus-like particles^{7,8} - potentiates the
30 cytotoxicity of Ara-C in AML cells. In mouse retroviral AML transplantation models as
31 well as in retrospective analyses of adult AML patients, the response to Ara-C-
32 containing therapy was inversely correlated with SAMHD1 expression. These results
33 identify SAMHD1 as a potential biomarker for the stratification of AML patients to
34 Ara-C-based therapy and as a target for treating Ara-C-refractory AML.

35
36

37 The current backbone of AML therapy is treatment with the cytidine analog Ara-C and the
38 anthracycline daunorubicin. Despite a high rate of initial remissions, a substantial fraction of
39 AML patients relapses and acquires resistance to Ara-C^{1,9}. The prognosis of AML patients,
40 especially elderly ones, remains dismal^{2,9}. Mutations in the *SAMHD1* gene, encoding Sterile
41 alpha motif and histidine-aspartic domain-containing protein 1 (SAMHD1), have been
42 associated with the Aicardi-Goutières autoimmune syndrome¹⁰ and the development of
43 malignancies including cutaneous T-cell lymphoma, chronic lymphatic leukemia, and colon
44 cancer¹¹⁻¹³. SAMHD1, a dNTP triphosphohydrolase that cleaves dNTPs into
45 deoxyribonucleosides and inorganic triphosphate, enhances the efficacy of certain nucleoside
46 analog drugs for the treatment of human immunodeficiency virus type-1 (HIV-1) by
47 decreasing the levels of intracellular dNTPs^{14,15}, which apparently compete with the
48 thymidine analog triphosphates for incorporation into HIV-1 cDNA during reverse
49 transcription¹⁶. We postulated that SAMHD1 could have a similar effect on nucleoside
50 analog-based therapy in leukemia⁶.

51 To investigate whether SAMHD1 expression enhances Ara-C cytotoxicity in AML
52 cells, we tested whether Ara-C sensitivity in 13 AML cell lines, determined by the half
53 maximal inhibitory concentration (IC_{50}), is correlated with SAMHD1 protein and mRNA
54 levels. Both SAMHD1 expression (**Fig. 1a** and **Supplementary Fig. 1**) and Ara-C sensitivity
55 (**Supplementary Table 1**) varied considerably among these cell lines. Unexpectedly,
56 SAMHD1 levels inversely correlated with Ara-C cytotoxicity ($p=0.0037$, **Fig. 1b** and
57 **Supplementary Fig. 2a,b**), as well as with the levels of early (Caspase 3 and 7 activity,
58 $p=0.02$, **Supplementary Fig. 3a,b**) and late (sub-G1 cells, apoptotic DNA fragmentation,
59 $p=0.029$, **Supplementary Fig. 3c,d**) markers of apoptosis. In contrast, no significant
60 correlation could be established between Ara-C IC_{50} values and the expression of cellular

61 proteins previously implicated in Ara-C uptake or its conversion to Ara-CTP¹, including
62 equilibrative nucleoside transporter (ENT1/SLC29A1), deoxycytidine kinase (DCK), cytidine
63 deaminase (CDA), deoxycytidilate deaminase (DCTD), or 5'-nucleotidase (NT5C2) (**Fig.**
64 **1a,c-g**).

65 To further investigate its role in Ara-C resistance, we tested the effects of SAMHD1
66 deficiency by a number of approaches: (i) depletion of SAMHD1 in AML cell lines
67 expressing high endogenous SAMHD1 levels using either lentiviral vectors encoding
68 *SAMHD1*-specific shRNA or transfection with *SAMHD1*-specific siRNA; (ii) CRISPR/Cas9-
69 mediated disruption of the *SAMHD1* gene; and (iii) targeted degradation of SAMHD1 using
70 virus-like particles (VLPs) which shuttle the SAMHD1-interacting lentiviral Vpx protein
71 (Vpx-VLPs) into cells^{7,8,17} (**Fig. 2a** and **Supplementary Fig. 4**). Vpx recruits SAMHD1 to a
72 cullin4A-RING E3 ubiquitin ligase (CRL4^{DCAF1}), which targets the enzyme for proteasomal
73 degradation^{7,8}.

74 *SAMHD1* depletion in AML cell lines by RNA interference (OCI-AML3, THP-1),
75 *SAMHD1* knockout (THP-1^{-/-}), or transduction with Vpx-VLPs (MonoMac6 cells, THP-1)
76 markedly sensitized AML cell lines to Ara-C toxicity relative to the respective controls (**Fig.**
77 **2a,b** and **Supplementary Fig. 4**). In contrast, *SAMHD1* siRNA had only a marginal effect on
78 Ara-C toxicity in low SAMHD1-expressing HEL cells (**Fig. 2a,b**). Interestingly, we observed
79 SAMHD1 dependency, although less pronounced, for the purine analog fludarabine
80 (**Supplementary Fig. 5a**); however, the IC₅₀ values for the topoisomerase II inhibitors
81 etoposide and daunorubicin, as well as for dFdC (2',2'-difluorodeoxycytidine; gemcitabine),
82 were not consistently affected by SAMHD1 down-modulation (**Supplementary Fig. 5b-d**),
83 indicating a certain degree of drug specificity.

84 In HEL cells, an AML cell line that expresses very low endogenous levels of
85 SAMHD1 (**Fig. 1a** and **Fig. 2a,c**), constitutive overexpression of wild-type SAMHD1
86 (SAMHD1-WT), but not of the dNTPase-deficient SAMHD1-D311A mutant, increased the
87 IC₅₀ values for Ara-C and fludarabine (**Fig. 2c** and **Supplementary Fig. 5a**). In contrast, the
88 toxicity of daunorubicin, etoposide, or dFdC was largely unaltered (**Supplementary Fig. 5b-**
89 **d**). These results indicate that SAMHD1's enzymatic activity is critically involved in
90 mediating resistance of AML cells to Ara-C and, to a lesser extent, fludarabine. Notably, Ara-
91 C at concentrations mimicking the steady state levels of Ara-C in plasma during standard Ara-
92 C regimens (100-200 mg/m²)¹ or the minimum blood plasma concentration (C_{min}; achieved
93 12h after completion of i.v. infusion) during high-dose Ara-C therapy (3000 mg/m²)¹⁸ only
94 partially affected the viability of SAMHD1-expressing AML cell lines, whereas SAMHD1-
95 depleted cells were effectively killed (**Supplementary Fig. 6**).

96 Although previous *in vitro* studies provided no evidence that triphosphorylated anti-
97 viral nucleoside analogs can be hydrolyzed by SAMHD1^{19,20}, we hypothesized that SAMHD1
98 might be able to hydrolyze Ara-CTP, which differs from the physiological dCTP substrate by
99 only a hydroxyl substituent in the up-position at carbon atom-2 of the pentose moiety
100 (**Supplementary Fig. 7**). To directly test whether Ara-CTP is hydrolyzed by SAMHD1, we
101 quantified Ara-CTP levels relative to SAMHD1 expression following short-term exposure of
102 AML cells to ¹³C₃-Ara-C, using liquid chromatography tandem mass spectrometry (LC-
103 MS/MS). We detected 47-fold higher Ara-CTP levels in SAMHD1-deficient THP-1^{-/-} cells
104 compared to THP-1^{+/+} control cells (**Supplementary Fig. 8a**), whereas SAMHD1 deficiency
105 did not affect dFd-CTP levels after drug treatment (**Supplementary Fig. 8b**). Moreover, HEL
106 SAMHD1-WT cells harbored 97- and 69-fold lower levels of Ara-CTP compared to parental
107 HEL cells and HEL cells expressing the SAMHD1-D311A mutant, respectively (**Fig. 2d**).

108 Notably, lack of enzymatically active SAMHD1 in THP-1^{-/-} cells or in parental and
109 SAMHD1-D311A-expressing HEL cells also resulted in elevated dNTP levels
110 (**Supplementary Fig. 9a,b**), which, however, did not counteract the cytotoxicity of the
111 concomitantly increased Ara-CTP levels (**Fig. 2b,c**).

112 dGTP or GTP binding to the primary allosteric site of SAMHD1 leads to formation of
113 a catalytically active tetramer, whereas the second allosteric site of the enzyme accommodates
114 dNTPs²¹⁻²³. To elucidate whether Ara-CTP can serve as a substrate or as both an activator and
115 substrate for the triphosphohydrolase, we performed an enzymatic *in vitro* assay using
116 bacterially expressed full-length SAMHD1. Analysis of reaction products by ion-pair reverse-
117 phase HPLC revealed that SAMHD1 hydrolyzes Ara-CTP to Ara-C, requiring the presence of
118 the activator dGTP, which itself is also cleaved to dG (**Fig. 2e**). In specificity control
119 experiments, the physiological substrate TTP, but not dFd-CTP, was hydrolyzed by SAMHD1
120 (**Supplementary Fig. 10a,b**). Thus, Ara-CTP is a direct substrate, but not an activator, of
121 SAMHD1's triphosphohydrolase activity in AML cells.

122 To explore whether SAMHD1 might contribute to the development of Ara-C
123 resistance, we gradually adapted three AML cell lines (HEL, HL-60, and Molm13),
124 characterized by low endogenous SAMHD1 expression levels and high Ara-C sensitivity, to
125 growth in the presence of the nucleoside analog. The resulting drug-resistant sublines were
126 cultivated in medium containing Ara-C at a concentration of 2 µg/ml (designated ^rAra-C^{2µg})
127 and displayed increases in Ara-C IC₅₀ values ranging from 1643- to 4250-fold relative to the
128 parental cell lines (**Supplementary Table 2**). In addition to changes in the expression of some
129 cellular factors previously implicated in acquired Ara-C resistance (i.e., DCK, CDA, and
130 NT5C2), the levels of SAMHD1 were markedly increased in the Ara-C-resistant sublines
131 relative to their parental counterparts (**Fig. 3a** and **Supplementary Fig. 11**). Ara-C resistance

132 was accompanied by drastically decreased Ara-CTP levels (**Fig. 3b**) and exposure of Ara-C-
133 resistant AML cells to Vpx-VLPs depleted SAMHD1, increased Ara-CTP levels, and re-
134 sensitized the cells to Ara-C by up to 11.5-fold relative to Vpr-VLP-treated control cells (**Fig.**
135 **3c,d**). Whereas cultivation of the parental AML cell lines in the presence of the drug for 24 h
136 did not acutely induce SAMHD1 levels (**Supplementary Fig. 12a**), selection for 20 d in
137 Molm13 cells resulted in an upregulation of SAMHD1 levels (**Supplementary Fig. 12b**).

138 To study the role of SAMHD1 in AML drug sensitivity *in vivo*, we transformed mouse
139 myeloid progenitor cells using the oncogenes Hoxa9/Meis1 or MN1 and subsequently deleted
140 the *SAMHD1* gene using CRISPR/Cas9 genome editing with two independent guide RNAs
141 (gRNA). *SAMHD1*^{+/+} control AML blasts and knockout (*SAMHD1*^{-/-}) AML blasts were
142 transplanted into irradiated recipient mice, and were treated with either Ara-C or phosphate-
143 buffered saline (PBS) on day 18 and 19 after transplantation (**Supplementary Fig. 13a-d**).
144 Overall survival of the two independent mouse cohorts transplanted with *SAMHD1*^{-/-} AML
145 was dramatically prolonged compared to *SAMHD1*^{+/+} AML by administration of Ara-C (**Fig.**
146 **4a,b** ($p=2.97\times 10^{-6}$ for both cohorts), **Supplementary Fig. 13e** ($p=3.05\times 10^{-6}$) and
147 **Supplementary Fig. 13f** ($p=4.32\times 10^{-6}$)), but not by PBS treatment (**Fig. 4a,b** and
148 **Supplementary Fig. 13e,f**). Similar results were obtained for two mouse cohorts for which a
149 second *SAMHD1* gRNA was used (**Supplementary Fig. 14**).

150 In human blasts isolated from bone marrow of therapy-naïve AML patients, basal
151 SAMHD1 expression correlated with Ara-C IC₅₀ values ($p=0.04$, **Supplementary Fig. 15**).
152 Moreover, we tested the effects of transient depletion of SAMHD1 in blasts of six patients
153 (**Supplementary Table 3**, patients A to F). Two days after transfection with control or
154 *SAMHD1*-targeting siRNA, the blasts were cultured in the presence of Ara-C or daunorubicin.
155 SAMHD1 depletion diminished Ara-C IC₅₀ values by 3- to 15-fold (**Fig. 4c**), whereas the

156 sensitivity of the blasts to daunorubicin was unaltered (**Supplementary Table 4**). Similarly,
157 treatment with SAMHD1-degrading Vpx-VLPs sensitized primary AML blasts to Ara-C, but
158 not to daunorubicin, compared to Vpr-containing control VLPs (**Supplementary Fig. 16** and
159 **Supplementary Table 5**). Concomitantly with this sensitization, intracellular Ara-CTP levels
160 were elevated (**Supplementary Fig. 8c,d**). Finally, we examined the suitability of SAMHD1
161 expression as a biomarker for predicting the response of AML to standard Ara-C-containing
162 therapy. We analyzed an AML cohort of 150 adult patients who had received one to two
163 courses of Ara-C-containing induction therapy in two University Hospital study centers in
164 Germany. Patients received either two cycles of “7+3” or “7+3” plus high-dose Ara-C in
165 combination with mitoxantrone (HAM) according to standard German AML protocols
166 (**Supplementary Table 6**). The “7+3” treatment regime refers to 7 days of standard-dose
167 Ara-C with the addition of daunorubicin for 3 days during the 7 day-chemotherapy induction
168 cycle (see Online Methods). Retrospective analysis of SAMHD1 protein levels by
169 immunohistochemical (IHC) staining of blasts in sections of paraffinized bone marrow
170 isolated at primary diagnosis revealed that expression of SAMHD1 was highly variable
171 between patients and, importantly, markedly increased in the group of AML patients that did
172 not reach a complete remission (“No CR”, n=38) at the end of induction therapy, as compared
173 to the group of patients with documented complete remission (“CR”, n=112) ($p=6.3\times 10^{-8}$,
174 Wilcoxon Rank Sum test) (**Fig. 4d,e** and **Supplementary Table 6**). Of the 150 patients, 112
175 achieved CR; of these 90 were scored as “SAMHD1-low” and 22 were scored as “SAMHD1-
176 high”. The CR rate in the “SAMHD1-high” cohort was 22/50 (44%), whereas the CR rate in
177 the “SAMHD1-low” cohort was 90/100 (90%). This difference between the two SAMHD1-
178 stratified cohorts was highly statistically significant ($p=3.477\times 10^{-9}$, Chi-Squared Test
179 with 1 degree of freedom). As a validation of the IHC staining and scoring system, levels of

180 SAMHD1 protein expression in blasts as determined by IHC scoring and in parallel by flow
181 cytometry showed a positive correlation ($p<0.0001$, **Supplementary Fig. 17b**). All CR
182 patients received post-remission therapy: a high-dose Ara-C-containing chemo-consolidation
183 regimen and/or allogeneic stem cell transplantation. In our AML cohort, the level of
184 SAMHD1 expression in blasts at initial diagnosis was highly predictive for event-free
185 survival (EFS) ($p=1.86\times 10^{-11}$, **Fig. 4f**), where an event was defined as failure to achieve CR,
186 relapse or death. Also, relapse-free survival (RFS) of CR patients was significantly worse in
187 “SAMHD1-high” compared to “SAMHD1-low” patients ($p=2.02 \times 10^{-4}$, **Fig. 4g**), indicating
188 that the depth of remission in “SAMHD1-high” patients was less pronounced than in
189 “SAMHD1-low” patients. Although the median observation time was relatively short,
190 “SAMHD1-high” patients experienced a significantly worse overall survival (OS) ($p=4.85$
191 $\times 10^{-3}$, **Fig. 4h**). When patients were censored from the analyses at the time of allogeneic
192 transplantation, all differences (EFS, RFS, OS) remained statistically significant
193 (**Supplementary Fig. 18a-c**). Notably, no correlation could be established between
194 cytogenetic risk groups and SAMHD1 expression (**Supplementary Fig. 19a**). In a
195 multivariate analysis including age, gender, initial leukocyte count and cytogenetic risk group,
196 and type of second induction cycle (HAM versus “7+3”), high SAMHD1 expression proved
197 to be an independent risk factor for EFS (hazard ratio 1.72, $p=5.23\times 10^{-8}$) and OS (1.33,
198 $p=0.0228$) (**Supplementary Fig. 19b,c**).

199 Furthermore, mining of the publicly available AML data set of the TCGA cohort²⁴
200 confirmed a correlation between low SAMHD1 mRNA expression with CR for patients who
201 had received an Ara-C-containing therapy (**Supplementary Fig. 20**). Thus, SAMHD1 levels
202 at diagnosis inversely correlate with the clinical response to Ara-C-based therapy in two

203 different adult AML patient cohorts, and this prominent role of SAMHD1 in Ara-C response
204 is corroborated by results from murine AML transplantation models.

205 Taken together, this study identifies SAMHD1 as a cellular biomarker for stratification
206 of patients to Ara-C-based therapy and uncovers a patient- and drug-specific interference
207 mechanism (**Supplementary Fig. 21**) that, in addition to established molecular and
208 cytogenetic risk factors²⁵, determines the outcome of AML disease. Ara-C's mimicry of the
209 physiological nucleoside cytidine endows it with anti-leukemic activity, but this mimicry is
210 detrimental in AML blasts that express the Ara-CTP-inactivating SAMHD1 protein. This
211 concept applies to a lesser extent also to the purine analog fludarabine, but not to dFdC,
212 indicating that SAMHD1 should be considered a critical cellular factor in the evaluation of all
213 nucleoside analog-based drugs or drug candidates in AML. Future studies will determine
214 whether protein- or mRNA-based quantification of SAMHD1 in AML blasts at diagnosis is a
215 better predictor of the therapeutic response. *In vivo* strategies aiming at transient
216 downregulation of SAMHD1 by either RNA interference or application of SAMHD1-
217 degrading Vpx-VLPs, or, conceivably, through administration of an inhibitor of SAMHD1's
218 enzymatic activity, may improve the Ara-C-based treatment of AML and other malignancies.

219

220 METHODS

221 Methods and any associated reference are available in the online version of the paper.

222 *Note: Any Supplementary Information and Source Data files are available in the online*
223 *version of the paper.*

224

225 Acknowledgements

226 This study to dedicated to the memory of Prof. Werner Reutter. We are grateful to Thomas
227 Gramberg and Irmela Jeremias for providing reagents. We thank Sebastian Grothe, Yvonne
228 Voges, and Kerstin Lehr for technical assistance, and Alessia Ruggieri for graphical art work.
229 We are grateful to Richard Zehner for STR profiling. We acknowledge logistic support by
230 Nikolas Herold for LC-MS/MS analyses in the period 09-11/2014 as scientific staff in the
231 laboratory of O.T.K. at Goethe University. F.C. is supported by an EMBO long-term
232 fellowship (1305-2015 and Marie Curie Actions LTFCOFUND2013/GA-2013-609409). The
233 WEBs laboratory is supported by the Deutsche Forschungsgemeinschaft grant DFG EXC
234 1003 (H.S.). This work was supported in part by the Medical Faculty of the University of
235 Frankfurt (O.T.K.), Hilfe für krebskranke Kinder Frankfurt e.V. (J.C.), the Frankfurter
236 Stiftung für krebskranke Kinder (J.C.), by the LOEWE Program of the State of Hessa
237 (LOEWE Center for Translational Medicine and Pharmacology, Frankfurt)(G.G. and H.S.),
238 the José Carreras Leukämie-Stiftung (J.C.), the Deutsche Forschungsgemeinschaft (KE 742/4-
239 1 (O.T.K.), SFB 1039/Z01 (G.G.)), the NSERC Strategic Network grant IBN (M.Mi.), the
240 Kent Cancer Trust (M.Mi.), and the LMU Munich (O.T.K.).

241

242 **Author Contributions**

243 J.C. and O.T.K. conceived the study and together with C.S., T.O., H.-M.B., and S.-M.S.
244 designed and analyzed the majority of experiments. D.T., R.F., H.B., L.S., M.Ma, and F.C.
245 conducted experiments, analyzed data, and provided discussion. A.C., J.L., M. Mi., and V.H.
246 provided critical reagents and discussion. G.G., M.-L.H., L.K., A.F.Y., P.S., N.F., C.S.,
247 W.E.B., W.H., E.W., and H.S. analyzed data and provided discussion. J.C. and O.T.K. wrote
248 and all authors edited the manuscript.

249 **Competing Financial Interests Statement**

250 The Johann Wolfgang Goethe-University has filed a patent application, on which several of
251 the coauthors are listed as inventors.

252

253 **References**

- 254 1. Lamba, J.K. Genetic factors influencing cytarabine therapy. *Pharmacogenomics* **10**,
255 1657-1674 (2009).
- 256 2. Burnett, A., Wetzler, M. & Lowenberg, B. Therapeutic advances in acute myeloid
257 leukemia. *J Clin Oncol* **29**, 487-494 (2011).
- 258 3. Lowenberg, B., *et al.* Cytarabine dose for acute myeloid leukemia. *N Engl J Med* **364**,
259 1027-1036 (2011).
- 260 4. Franzolin, E., *et al.* The deoxynucleotide triphosphohydrolase SAMHD1 is a major
261 regulator of DNA precursor pools in mammalian cells. *Proc Natl Acad Sci U S A* **110**,
262 14272-14277 (2013).
- 263 5. Li, N., Zhang, W. & Cao, X. Identification of human homologue of mouse IFN-
264 gamma induced protein from human dendritic cells. *Immunol Lett* **74**, 221-224 (2000).
- 265 6. Kohnken, R., Kodigeppalli, K.M. & Wu, L. Regulation of deoxynucleotide metabolism
266 in cancer: novel mechanisms and therapeutic implications. *Mol Cancer* **14**, 176
267 (2015).
- 268 7. Hrecka, K., *et al.* Vpx relieves inhibition of HIV-1 infection of macrophages mediated
269 by the SAMHD1 protein. *Nature* **474**, 658-661 (2011).
- 270 8. Laguette, N., *et al.* SAMHD1 is the dendritic- and myeloid-cell-specific HIV-1
271 restriction factor counteracted by Vpx. *Nature* **474**, 654-657 (2011).
- 272 9. Dombret, H. & Gardin, C. An update of current treatments for adult acute myeloid
273 leukemia. *Blood* **127**, 53-61 (2016).
- 274 10. Crow, Y.J. & Rehwinkel, J. Aicardi-Goutieres syndrome and related phenotypes:
275 linking nucleic acid metabolism with autoimmunity. *Hum Mol Genet* **18**, R130-136
276 (2009).
- 277 11. Clifford, R., *et al.* SAMHD1 is mutated recurrently in chronic lymphocytic leukemia
278 and is involved in response to DNA damage. *Blood* **123**, 1021-1031 (2014).
- 279 12. Merati, M., *et al.* Aggressive CD8(+) epidermotropic cutaneous T-cell lymphoma
280 associated with homozygous mutation in SAMHD1. *JAAD Case Rep* **1**, 227-229
281 (2015).
- 282 13. Rentoft, M., *et al.* Heterozygous colon cancer-associated mutations of SAMHD1 have
283 functional significance. *Proc Natl Acad Sci U S A* (2016).
- 284 14. Lahouassa, H., *et al.* SAMHD1 restricts the replication of human immunodeficiency
285 virus type 1 by depleting the intracellular pool of deoxynucleoside triphosphates. *Nat
286 Immunol* **13**, 223-228 (2012).
- 287 15. Baldauf, H.M., *et al.* SAMHD1 restricts HIV-1 infection in resting CD4(+) T cells.
288 *Nat Med* **18**, 1682-1687 (2012).

- 289 16. Ballana, E., *et al.* SAMHD1 specifically affects the antiviral potency of thymidine
290 analog HIV reverse transcriptase inhibitors. *Antimicrob Agents Chemother* **58**, 4804-
291 4813 (2014).
- 292 17. Gramberg, T., Sunseri, N. & Landau, N.R. Evidence for an activation domain at the
293 amino terminus of simian immunodeficiency virus Vpx. *J Virol* **84**, 1387-1396 (2010).
- 294 18. Early, A.P., Preisler, H.D., Slocum, H. & Rustum, Y.M. A pilot study of high-dose 1-
295 beta-D-arabinofuranosylcytosine for acute leukemia and refractory lymphoma: clinical
296 response and pharmacology. *Cancer Res* **42**, 1587-1594 (1982).
- 297 19. Arnold, L.H., Kunzelmann, S., Webb, M.R. & Taylor, I.A. A continuous enzyme-
298 coupled assay for triphosphohydrolase activity of HIV-1 restriction factor SAMHD1.
299 *Antimicrob Agents Chemother* **59**, 186-192 (2015).
- 300 20. Huber, A.D., *et al.* SAMHD1 has differential impact on the efficacies of HIV
301 nucleoside reverse transcriptase inhibitors. *Antimicrob Agents Chemother* **58**, 4915-
302 4919 (2014).
- 303 21. Goldstone, D.C., *et al.* HIV-1 restriction factor SAMHD1 is a deoxynucleoside
304 triphosphate triphosphohydrolase. *Nature* **480**, 379-382 (2011).
- 305 22. Koharudin, L.M., *et al.* Structural basis of allosteric activation of sterile alpha motif
306 and histidine-aspartate domain-containing protein 1 (SAMHD1) by nucleoside
307 triphosphates. *J Biol Chem* **289**, 32617-32627 (2014).
- 308 23. Yan, J., *et al.* Tetramerization of SAMHD1 is required for biological activity and
309 inhibition of HIV infection. *J Biol Chem* **288**, 10406-10417 (2013).
- 310 24. Genome, C. Genomic and epigenomic landscapes of adult de novo acute myeloid
311 leukemia. *N Engl J Med* **368**, 2059-2074 (2013).
- 312 25. Komanduri, K.V. & Levine, R.L. Diagnosis and Therapy of Acute Myeloid Leukemia
313 in the Era of Molecular Risk Stratification. *Annu Rev Med* **67**, 59-72 (2016).

315 **Legends to Figures**

316

317 **Figure 1 | SAMHD1 expression levels inversely correlate with Ara-C cytotoxicity in**
318 **AML cell lines.** **(a)** Representative immunoblots of SAMHD1 and other proteins previously
319 reported to be involved in Ara-C uptake and its conversion to the active Ara-C metabolite,
320 Ara-CTP, in the indicated AML cell lines. β-actin served as a loading control. Three
321 independent experiments were performed. Uncropped images are shown in **Supplementary**
322 **Figure 22.** **(b-g)** Correlation analyses between Ara-C IC₅₀ values for these AML cell lines in
323 **a** and the relative expression levels of SAMHD1 **(b)**, ENT1 **(c)**, DCK **(d)**, CDA **(e)**, DCTD
324 **(f)**, or NT5C2 **(g)**. Expression levels were normalized to β-actin and are shown as arbitrary
325 units (a.u.); the relative expression of each protein in THP-1 cells was set to 1. For **b-g**, closed
326 circles and error bars represent mean ± s.e.m. of three independent experiments each
327 performed with technical replicates (n=3). Data in **b-g** were analysed using a linear regression
328 model. R² values indicate goodness of fit of the regression model to the data, and represent
329 variance explained by the independent variable divided by total variance of the IC₅₀ Ara-C
330 values.

331

332 **Figure 2 | SAMHD1 counteracts Ara-C toxicity in AML cell lines via hydrolysis of the**
333 **active metabolite, Ara-CTP.** **(a)** Representative immunoblots for SAMHD1 after
334 CRISPR/Cas9-mediated *SAMHD1* knockout in THP-1 (THP-1^{-/-}) cells or after shRNA or
335 siRNA-mediated silencing of *SAMHD1* in OCI-AML3 and HEL cells. Alternatively, OCI-
336 AML3 and MonoMac6 cells were transduced with VLPs carrying either lentiviral Vpr (Vpr-
337 VLPs, control) or Vpx (Vpx-VLPs) proteins. β-actin served as a loading control. Uncropped
338 images are shown in **Supplementary Figures 22 and 23.** **(b)** Ara-C IC₅₀ values of the

339 experimental groups shown in **a**. Each circle represents a technical replicate (n=3) of three
340 independent experiments performed. Horizontal lines and error bars represent means \pm s.e.m.
341 Numbers at the top indicate the factor of decrease of Ara-C IC₅₀ values in SAMHD1-depleted
342 relative to control cells. **(c)** Ara-C IC₅₀ values (top) and immunoblot for SAMHD1 (bottom)
343 in parental HEL cells or HEL cells stably transduced with either wildtype SAMHD1
344 (SAMHD1-WT) or the dNTPase-inactive D311A SAMHD1 mutant (SAMHD1-D311A). For
345 the IC₅₀ data, the numbers above the bars indicate the factor by which the IC₅₀ value differed
346 relative to HEL SAMHD1-WT cells. The IC₅₀ values are shown as means \pm s.e.m. of three
347 independent experiments each performed with technical replicates (n=3) represented by
348 individual circles. β -actin served as a loading control for the SAMHD1 immunoblot.
349 Uncropped images are shown in **Supplementary Figure 23**. **(d)** Representative liquid
350 chromatography tandem mass spectrometry (LC-MS/MS) analysis of Ara-CTP in parental
351 HEL cells (blue chromatogram), HEL SAMHD1-WT cells (black chromatogram), or HEL
352 SAMHD1-D311A cells (red chromatogram). **(e)** HPLC analysis of products from an
353 enzymatic *in vitro* assay using bacterially expressed full-length SAMHD1. Ara-CTP was
354 incubated by itself (top), in the presence of SAMHD1 (middle), or in the presence of
355 SAMHD1 and the allosteric activator/substrate dGTP (bottom). Chromatogram peaks
356 corresponding to Ara-C, dG, and Ara-CTP are indicated. Statistical analyses were performed
357 using unpaired two-tailed Students' *t*-test. For **(b)** the degree of freedom was 16 and p<
358 0.0001 for all except for siRNA-treated HEL cells (df =4, p=0.0004). df was 16 and p<
359 0.0001 for **(c)**. *p≤0.05; **p<0.01, ***p<0.001.

360

361

362

363 **Figure 3 | SAMHD1 contributes to the acquired resistance of AML cells to Ara-C. (a)**
364 Representative immunoblots of proteins involved in Ara-C uptake and metabolism in parental
365 AML cell lines (HEL, HL-60, and Molm13) and in their respective Ara-C-resistant sublines
366 ($\text{HEL}^r\text{Ara-C}^{2\mu\text{g}}$, $\text{HL-60}^r\text{Ara-C}^{2\mu\text{g}}$, and $\text{Molm13}^r\text{Ara-C}^{2\mu\text{g}}$). β -actin served as a loading control.
367 Three independent experiments were performed. Uncropped images are shown in
368 **Supplementary Figure 24.** (b) Quantitative analysis by LC-MS/MS of Ara-CTP levels in
369 parental and Ara-C-resistant AML cell lines. The means \pm s.d. of triplicates of one
370 representative experiment are shown; three independent experiments were performed.
371 Numbers above the bars represent the factor of decrease in Ara-CTP levels in Ara-C-resistant
372 cell lines relative to their parental counterparts. (c) Ara-C-resistant cell lines were treated with
373 the indicated VLPs and subsequently analyzed for Ara-C cytotoxicity (top) and SAMHD1
374 expression (bottom). Ara-C IC₅₀ values of three independent experiments each performed
375 with technical replicates (n=3) are presented with center lines showing the medians. The box
376 limits are quartiles 1 and 3, and whiskers show maximum and minimum values. Numbers
377 above the bars indicate the factor of decrease in IC₅₀ values in Vpx-VLP-treated cells relative
378 to Vpr-VLP-treated controls. (d) Representative LC-MS/MS chromatograms of Ara-CTP in
379 Molm13^rAra-C^{2μg} cells treated with either Vpr-VLPs (control, black), Vpx-VLPs (red), or left
380 untreated (blue). Statistical analyses were performed using unpaired two-tailed Students' *t*-
381 test. For (b) the degree of freedom for all was 4 and exact p-values 0.0073 for HEL cells,
382 0.0037 for HL-60 cells and 0.0004 for Molm13 cells. df was 16 and p< 0.0001 for
383 (c). *p≤0.05; **p<0.01, ***p <0.001.

384
385 **Figure 4 | SAMHD1 expression in leukemic blasts predicts response to Ara-C-**
386 **containing therapy in mouse transplantation models and AML patients. (a,b)** Kaplan-

387 Meier survival analyses of Hoxa9/Meis1- (**a**) or MN1-driven (**b**) AML transplantation models
388 using myeloid progenitors with endogenous SAMHD1 expression (SAMHD1^{+/+}) or
389 SAMHD1-deleted (SAMHD1^{-/-}) myeloid progenitors. Ara-C: i.p. administration of 75 mg/kg
390 Ara-C on days 18 and 19 after transplantation; Control: PBS. The difference in overall
391 survival between Ara-C-treated SAMHD1^{+/+} and SAMHD1^{-/-} mice was statistically significant
392 (logrank test, Hoxa9/Meis1: $p=2.97 \times 10^{-6}$, n=10 both groups; MN1: $p=2.97 \times 10^{-6}$, n=10 both
393 groups). The differences between the two control groups and between SAMHD1^{+/+} Ara-C and
394 both control groups were not significant (Hoxa9/Meis1: $p=0.42$, SAMHD1^{-/-} (n=10) vs
395 SAMHD1^{+/+} (n=9); MN1: $p=0.196$, n=10 both groups). **(c)** Blasts isolated from bone marrow
396 from six adult AML patients (A–F) were transfected with *SAMHD1*-specific or control
397 siRNAs and two days later analyzed for Ara-C cytotoxicity (top) and SAMHD1 expression
398 (bottom). Ara-C IC₅₀ values are presented as the means ± s.d. of the triplicates shown. The
399 numbers above the data points indicate the factor of difference between the siCTRL and
400 si*SAMHD1* groups. Uncropped images are shown in **Supplementary Figure 25**. **(d)**
401 Representative IHC micrographs showing SAMHD1 and CD34 expression in bone marrow
402 (BM) from one No CR patient (#39), one CR patient (#28), and one healthy donor. Scale bar:
403 50 μm. **(e)** Comparison of SAMHD1 expression levels (IHC scores) in CR and No CR
404 patients. See Online Methods for an explanation of the IHC scores. Shown are relative
405 frequencies (in percent) of patients with IHC scores of 0, 1, 2 or 3 among CR (n=112) and No
406 CR (n=38) patients. **f-h**, Kaplan-Meier analyses for event-free survival (**f**), relapse-free
407 survival (**g**), and overall survival (**h**), for which AML patients were grouped into “No / low
408 SAMHD1 expressors” (IHC scores 0 or 1, red curves) versus “High SAMHD1 expressors”
409 (IHC scores 2 or 3, black curves). Numbers above the plots indicate the absolute number of
410 patients in each of the two groups at the respective time points. Significance of difference

411 between survival curves in **f,g,h** was assessed using the logrank test (p-values indicated in
412 figure).

413

414 **ONLINE METHODS**

415 **Ethics statement.** Whole blood and bone marrow biopsies of AML patients were obtained
416 and collected pre- and post-treatment. All patients gave informed consent according to the
417 Declaration of Helsinki to participate in the collection of samples. The use of whole blood and
418 bone marrow aspirates was approved by the Ethics Committee of Frankfurt University
419 Hospital (approval no. SPO-01-2015) and University Hospital Münster (approval no. 2007-
420 390-f-S).

421

422 **Plasmids.** The SIVmac251-based *gag-pol* expression constructs pSIV3+R- (Vpr-deficient)
423 and pSIV3+X- (Vpx-deficient) were previously reported¹⁷. pLKO.1-puro-control-shRNA and
424 pLKO.1-puro-SAMHD1-shRNA#1-3 for shRNA-mediated silencing of SAMHD1 were
425 previously described¹⁵. pHr-based transfer vectors expressing SAMHD1-WT or the D311A
426 mutant were generated by site-directed mutagenesis in a codon-optimized SAMHD1
427 expression construct (kindly provided by Dr. Thomas Gramberg, Institute of Clinical and
428 Molecular Virology, FAU Erlangen-Nürnberg, Erlangen, Germany) and subcloned into pHr-
429 luc transfer vectors. pPAX2 was purchased from Addgene and pVSV-G has been previously
430 described²⁶.

431

432 **Cells and Reagents.** Human AML cell lines including THP-1 (DSMZ no. ACC16; FAB M6),
433 OCI-AML2 (DSMZ No. ACC 99; FAB M4), OCI-AML3 (DSMZ No. ACC 582; FAB M4),
434 Molm13 (DSMZ No. ACC 554; FAB M5a), PL-21 (DSMZ No. ACC 536; FAB M3), HL-60

435 (DSMZ No. ACC 3; FAB M2), MV4-11 (DSMZ No. ACC 102; FAB M5), SIG-M5 (DSMZ
436 No. ACC 468; FAB M5a), ML2 (DSMZ No. ACC 15; FAB M4), NB4 (DSMZ No. ACC
437 207; FAB M3), KG1 (DSMZ No. ACC 14; FAB not indicated), MonoMac6 (DSMZ No.
438 ACC 124; FAB M5), and HEL (DSMZ No. ACC 11; FAB M6) were obtained from DSMZ
439 (Deutsche Sammlung von Mikroorganismen und Zellkulturen GmbH). All cell lines were
440 cultured in IMDM (Biochrom) supplemented with 10% FBS (SIG-M5 20% FBS), 4 mM L-
441 Glutamine, 100 IU/ml penicillin, and 100 mg/ml streptomycin at 37°C in a humidified 5 %
442 CO₂ incubator. Cells were routinely tested for mycoplasma contamination (LT07-710, Lonza)
443 and authenticated by short tandem repeat profiling, as reported²⁷. THP-1 cells deficient for
444 SAMHD1 (THP-1^{-/-}) and control cells (THP-1^{+/+}) were generated as previously described²⁸
445 and cultivated in RPMI supplemented with 10% FCS, 100 IU/ml penicillin, and 100 mg/ml
446 streptomycin.

447 Mononuclear cells from blood or bone marrow AML samples were purified by Ficoll-
448 Hypaque gradient centrifugation²⁶. Leukemic cells were enriched by negative selection with a
449 combination of CD3- (130-150-101), CD19- (130-150-301) and CD235a-microbeads (130-
450 150-501, all from Miltenyi Biotec) according to the manufacturer's instructions and separated
451 by the autoMACS™ Pro Separator. All preparations were evaluated for purity resulting in
452 >90% leukemic blasts. The AML-393 sample carrying a MLL-AF10 translocation was
453 derived from a 47 year old female with AML at relapse after bone marrow transplantation.
454 Primary cells were amplified in NSG mice and re-isolated from enlarged spleens as
455 described²⁹. Frozen cells were kindly provided by Dr. Irmela Jeremias (Department of Gene
456 Vectors, Helmholtz Zentrum München, German Research Center for Environmental Health,
457 Munich, Germany) and thawed for experiments.

458 AML blasts (2×10^6) were cultivated in X-vivo 10 medium (Lonza) supplemented with 10%
459 HyClone FCS (Perbio), 4 mM L-glutamine, 25 ng/ml hTPO (130-094-013), 50 ng/ml hSCF
460 (130-096-695), 50 ng/ml hFlt3-Ligand (130-096-479) and 20 ng/ml hIL3 (130-095-069, all
461 from Miltenyi Biotec) in 96-well plates in the presence or absence of drugs.
462 The ecotropic GP+E86 packaging cell line was cultured in DMEM (Life Technologies) with
463 10% heat-inactivated FCS, 2 mM L-Glutamine, 100 U/ml Penicillin and 100 µg/ml
464 Streptomycin. Murine bone marrow cells were cultured in DMEM with 10% heat-inactivated
465 FCS, 2 mM L-Glutamine, 100 U/ml Penicillin and 100 µg/ml Streptomycin supplemented
466 with 10ng/ml murine recombinant IL3 (213-13), 10 ng/ml human recombinant IL6 (200-06),
467 and 100ng/ml murine recombinant SCF (250-03) (all from Peprotech).
468 Ara-C was purchased from Tocris (147-94-4), daunorubicin from Selleckchem (S3035),
469 etoposide from TEVA (45891.00), fludarabine from Tocris (21679-14-1) and dFdC
470 (gemcitabine) from Accord Healthcare GmbH (82092.00.00). Deoxynucleosides (dNs)
471 (Sigma-Aldrich), which are dNTP precursors, were used as previously reported¹⁵. All
472 nucleotide standards and internal standards for the LC-MS/MS analysis were obtained from
473 Sigma-Aldrich, Silantes or Alsachim³⁰. Labeled cytarabine, ¹³C₃-Ara-C (SC-217994, Santa
474 Cruz), was used for LC-MS/MS analysis.

475
476 **Generation of Ara-C-resistant cell lines.** Ara-C-resistant cell lines were established by
477 continuous exposure of Ara-C sensitive cell lines HL-60, HEL, Molm13, THP-1, MV4-11,
478 OCI-AML3 to increasing drug concentrations as previously described^{31,32} and are part of the
479 Resistant Cancer Cell Line (RCCL) collection
480 (<http://www.kent.ac.uk/stms/cmp/RCCL/RCCLabout>). Briefly, cells were cultured at
481 increasing Ara-C concentrations starting with concentrations that inhibited viability of the

482 parental cell lines by 50 % (IC_{50}). Ara-C concentrations were doubled every 2 to 6 weeks until
483 cells readily grew in the presence of 2 μ g Ara-C. Resistant cell lines were designated as HL-
484 60^rAra-C^{2 μ g}, HEL^rAra-C^{2 μ g}, Molm13^rAra-C^{2 μ g}, THP-1^rAra-C^{2 μ g}, MV4-11^rAra-C^{2 μ g} and OCI-
485 AML3^rAra-C^{2 μ g} and were continuously cultured in the presence of 2 μ g Ara-C. Cells were
486 routinely tested for mycoplasma contamination (LT07-710, Lonza) and authenticated by short
487 tandem repeat profiling²⁷.

488

489 **Cell viability assay.** The viability of AML cell lines treated with various drug concentrations
490 was determined by the 3-(4,5-dimethylthiazol-2-yl)-2,5-diphenyltetrazolium bromide (MTT)
491 dye reduction assay after 96 hours of incubation as described previously³³. IC_{50} values were
492 determined using CalcuSyn (Biosoft).

493

494 **Cytotoxic assay for AML blasts *ex vivo*.** The cell viability of AML blasts was determined
495 after 96 hours of incubation by the quantification of ATP levels in cell culture supernatants
496 using the CellTiter-Glo® Luminescent Cell Viability Assay (G7573, Promega) according to
497 the manufacturer's instructions. Luminescence was measured on a Tecan infinite M200
498 (TECAN) instrument at a wavelength of 560 nm (reference wavelength 620 nm). IC_{50} values
499 were determined using CalcuSyn (Biosoft).

500

501 **Apoptosis assays.** Sub-G1 cells as a marker for DNA fragmentation in late apoptotic cells
502 were measured according to Nicoletti by flow cytometry³⁴. Briefly, Ara-C-treated and
503 untreated cells were washed once in 1x PBS, incubated for at least 2h at 4°C with Nicoletti
504 buffer (0.1 % trisodiumcitrate-dihydrate pH 7.4, 0.1% Triton X-100, 50 μ g/ml propidium
505 iodide), and diluted prior to measurement in 1x PBS. Samples were analyzed using a

506 FACSVerse (BD Biosciences) and FlowJo software (TreeStar). Alternatively, Caspase 3/7
507 activity as a surrogate for early apoptosis was quantified by luminescence. Briefly, Ara-C-
508 treated and untreated cells were measured using the Caspase-Glo® 3/7 assay (G8091,
509 Promega) according to the manufacturer's instructions. Luminescence was measured on a
510 Tecan infinite M200 (TECAN) instrument at a wavelength of 560 nm (reference wavelength
511 620 nm).

512

513 **Flow cytometry.** Intracellular SAMHD1 staining was performed as previously described¹⁵.
514 Staining for surface markers (CD33, CD34, CD45) was applied prior to fixation. The
515 following fluorochrome-conjugated antibodies were used: CD33-PE (130-091-732), CD34-
516 FITC (130-081-001, both from Miltenyi Biotech), and CD45-V450 (560373, BD
517 Pharmingen), all diluted 1:11 per 10^7 cells, and Alexa-Fluor-660 (A-21074, Invitrogen, Life
518 technologies, 1:200). Samples were analyzed using a FACSVerse or FACSCanto II flow
519 cytometer (BD Biosciences) and FlowJo software (TreeStar).

520 For *in vitro* characterization of Hoxa9/Meis1- and MN1-transformed myeloid progenitor cells,
521 surface-marker expression was characterized by flow cytometry using a LSRII Fortessa flow
522 cytometer (BD Biosciences). Briefly, cells (2×10^5) were washed twice with 2% FCS in PBS
523 and stained with the following antibodies: PerCP-Cy5.5-conjugated anti-mouse Gr1 (45-
524 5931), V450-conjugated anti-mouse Mac1 (48-0112), APC-conjugated anti-mouse c-kit (17-
525 1171), PE-Cy7-conjugated anti-mouse Sca1 (25-5981), PE-conjugated anti-mouse FcεRI (12-
526 5898, all from eBioscience), and APC-H7-conjugated anti-mouse CD19 (560245, BD
527 Bioscience). 7-AAD (BD-Bioscience) was used for exclusion of dead cells.

528

529 **Immunoblotting.** Cells were lysed in Triton X-100 sample buffer and proteins separated by
530 sodium dodecyl sulfate-polyacrylamide gel electrophoresis. Proteins were blotted onto a
531 nitrocellulose membrane (Thermo Scientific). The following primary antibodies were used at
532 the indicated dilutions, SAMHD1 (12586-1-AP, Proteintech, 1:1000), β-actin (3598R-100,
533 BioVision via BioCat, 1:2000), DCK (sc-393099, Santa Cruz, 1:500), CDA (sc-365292, Santa
534 Cruz, 1:100), ENT1 (ab135756, Abcam, 1:500), and NT5C2 (H00022978-M02, Abnova,
535 1:200), DCTD (NBP1-75825, Novus, 1:200). Visualization and quantification was performed
536 using fluorescently labeled secondary antibodies (926-32210 IRDye® 800CW Goat anti-
537 Mouse and 926-32211 IRDye® 800CW Goat anti-Rabbit, LI-COR, 1:20000) and an Odyssey
538 CLx Imaging system (LI-COR Biosciences).

539

540 **Patients.** Patients were admitted to the University Hospital Frankfurt between 2010 and 2014
541 and treated for newly diagnosed AML with regimens containing standard dose Ara-C and
542 daunorubicin (“7+3”) (83 patients) or Ara-C alone (1 patient) (**Supplementary Table 6**); an
543 additional 66 patients admitted to the University Hospital Münster were included in the IHC
544 analyses. In addition, viable AML cells were purified from bone marrow of patients that were
545 admitted to the University Hospital Frankfurt in 2015 and 2016 (**Supplementary Table 3**).
546 Patients at the University Hospitals of Frankfurt and Münster are routinely advised to undergo
547 a bone marrow biopsy at diagnosis. All patients consented to the scientific analyses of their
548 data and to scientific analyses of biomaterial that was obtained for diagnostic purposes. All
549 patients received at least one course of Ara-C at a dose of 100 mg/m² over 7 days and
550 daunorubicin at a dose of 60 mg/m² over 3 days (“7+3”) (if not otherwise stated). All patients
551 below the age of 60 received a second cycle of induction therapy. Patients over the age of 60
552 received a second induction cycle only if their day 15 bone marrow aspirate showed more

553 than 5% blasts. For the analyses, patient records were reviewed by physicians who were
554 unaware of the SAMHD1 expression results in the diagnostic biopsies. Remission criteria and
555 cytogenetic risk groups were assessed according to the ELN guidelines.

556 The initial response to induction therapy was analyzed in bone marrow biopsies/aspirates and
557 defined as complete (CR) if the blast count was <5%, and as “No CR” if the blast count was
558 >5%. For the calculation of event-free survival (EFS), events were defined as failure to
559 achieve complete remission (CR, CRi, CRp) within 40 days after the last induction cycle,
560 relapse, or death at any time after start of therapy. Relapse-free survival (RFS) and remission
561 duration were calculated only in patients that achieved CR.

562

563 **Immunostaining of bone marrow samples.** Bone marrow samples from 154 patients,
564 including 150 AML patients and four healthy donors, were provided by the University
565 Hospital Frankfurt and University Hospital Münster, Germany. Tissues were fixed in 4%
566 buffered formalin, descaled by EDTA and embedded in paraffin. Immunohistochemical
567 staining was performed as previously described³⁵. Briefly, 2-μm bone marrow tissue sections
568 were incubated with EnVision Flex Target Retrieval Solution, pH low (K8005, DAKO) and
569 stained with primary antibodies directed against SAMHD1 (12586-1-AP, Proteintech, 1:3000)
570 and against CD34 (IR632, DAKO) for 40 min at room temperature. Polymeric secondary
571 antibodies coupled to HRPO peroxidase and DAB were used for visualization (REAL
572 EnVision Peroxidase/DAB+, K5007, DAKO). Tissue samples were analyzed by light
573 microscopy after counterstaining with Meyer’s haematoxylin (K8008, DAKO).

574 Two pathologists, who were blinded to clinical history and therapeutic response,
575 independently scored the SAMHD1 IHCs. They evaluated all tissue sections for nuclear
576 SAMHD1 staining using a four-stage staining score: 0 = negative, 1 = weak intensity of

577 staining, 2 = strong intensity of staining in less than 25% of blasts, 3 = strong intensity of
578 staining in more than 25% of blasts. IHC staining scores of 0 and 1 were defined as “No / low
579 expression” and IHC staining scores of 2 and 3 were defined as “High SAMHD1 expression”.
580 Membranous CD34 staining for the quantification of the number of AML blasts was
581 evaluated using a two-stage staining score: 0 = negative, 1 = positive.

582

583 **Retrospective analysis of the TCGA AML cohort.** Clinical data, mutational profiles and
584 normalized gene expression data for a cohort of 200 AML patients from The Cancer Genome
585 Atlas (TCGA, run date 20150821)²⁴ were retrieved using the RTCGA-Toolbox
586 R/BioConductor package, version 2.2.2³⁶. All analyses were performed using R 3.3.0 and
587 custom scripts. To test the association between SAMHD1 expression and first complete
588 remission, all Ara-C-treated patients with available gene expression data were considered. To
589 test the association between SAMHD1 expression and cytogenetic risk, all patients with
590 available gene expression data were considered. For analysis of mutation rates, all patients
591 with available mutational profiles were considered.

592

593 **Mice and retroviral infection of lineage-depleted bone-marrow cells.** C57BL/6J female
594 mice (age: 8-12 weeks) were obtained from Janvier-Labs (Le Genest-Saint-Isle, France). All
595 animal experiments were performed according to the regulations of the United Kingdom
596 Home Office and German authorities. All animal experiments were performed according to
597 national and international standards. Bone marrow cells were harvested from mice, and
598 lineage-negative cells were obtained by negative selection using the Lineage Cell Depletion
599 Kit (130-090-858, Miltenyi Biotec) as recommended by the manufacturer. Lineage-negative
600 cells were co-cultured with GP+E86 cells packaging MSCV-Hoxa9-PGK-neo in the presence

601 of polybrene (10 µg/ml, Sigma-Aldrich) for 3 days followed by co-incubation with GP+E86
602 MSCV-Meis1-IRES-YFP for 1 day. Hoxa9-expressing cells were selected with 0.6 mg/ml
603 G418 (Sigma-Aldrich) for at least 5 days. MN1-overexpressing myeloid progenitor cells were
604 generated as described previously³⁷. After selection, cells were sorted with a FACS BD Aria
605 III cell sorter. Lentiviral transductions of cultured cells with pLentiCRISPRv2 vectors
606 encoding *SAMHD1*-specific CRISPR or control vectors were performed as described
607 previously³⁵ using BU033 (5' CACCGgacgttcatccaaaa 3') and BU034 (5'
608 AACttttggatgaggatcgC 3') (**Fig. 4a,b**), or BU035 (5' CACCGgatgttctgataaggaga 3') and
609 BU036 (5' AACtctcattcagaatcatcC 3') (**Supplementary Fig. 14**).

610

611 **Transplantation and monitoring analyses of transplanted mice.** 7.5×10^4 cells were
612 transplanted together with 2×10^5 “support cells” by injection into the tail vein of lethally
613 irradiated (9.5 Gy) recipient mice (C57BL/6J). Wild-type mononuclear bone marrow cells
614 isolated from C57BL/6J mice and purified on a Ficoll gradient (Sigma-Aldrich) were used as
615 support cells to reconstitute hematopoiesis in irradiated recipient mice. 18 days after
616 transplantation, mice were treated with 75 mg/kg cytarabine or PBS (i.p.) for 2 subsequent
617 days.

618 Blood and bone marrow cells were isolated from mice for further analyses. Blood counts were
619 analyzed with ScilVet abc animal blood cell counter (Scil Animal Care Company). Cells from
620 spleen and bone marrow were incubated for 10 min with erythrocyte lysis buffer (155 mM
621 NH₄Cl, 10 mM KHCO₃, 0.1 mM EDTA) and then washed twice with 2% FCS in PBS.
622 Staining was performed as described above.

623 Blood smears and purified cells from bone marrow and spleen were centrifuged on cover slips
624 (2×10^5 cells/slip). Subsequently, cells were fixed for 10 min with methanol and stained with a

625 May-Grünwald solution for 8 min followed by Giemsa (both Merck Millipore) staining for 20
626 min.

627

628 **mRNA analyses.** RNA extraction and TaqMan-based mRNA quantification of SAMHD1
629 (Applied Biosystems: assay no. Hs00210019-m1) and RNaseP (Applied Biosystems:
630 TaqMan® RNase P Control Reagents Kit (4316844), endogenous reference control) were
631 performed essentially as reported³⁸.

632

633 **LC-MS/MS analysis.** Cells (5×10^5) were treated with 10 $\mu\text{g}/\text{ml}$ $^{13}\text{C}_3\text{-Ara-C}$ (SC-217994,
634 Santa Cruz) and incubated at 37°C in a humidified 5 % CO₂ incubator for 6 h. Subsequently,
635 cells were washed twice in 1 ml PBS, pelleted and stored at -20°C until measurement. The
636 concentrations of dNTPs, $^{13}\text{C}_3\text{-Ara-CTP}$, and dFdC-TP in the samples were analyzed by
637 liquid chromatography-electrospray ionization-tandem mass spectrometry essentially as
638 previously described³⁰. Briefly, the analytes were extracted by protein precipitation with
639 methanol. An anion exchange HPLC column (BioBasic AX, 150 x 2.1 mm, Thermo) was used
640 for the chromatographic separation and a 5500 QTrap (Sciex) instrument was used to
641 analyze the samples, operating as triple quadrupole in positive multiple reaction monitoring
642 (MRM) mode. Analysis of dNTPs was performed as previously described³⁰. Additionally,
643 $^{13}\text{C}_3\text{-Ara-CTP}$ and dFdC-TP were quantified using Cytidine- $^{13}\text{C}_9, ^{15}\text{N}_3\text{-5}'\text{-triphosphate}$ as an
644 internal standard (IS). The precursor-to-product ion transitions used as quantifiers were *m/z*
645 487.0 → 115.1 for $^{13}\text{C}_3\text{-Ara-CTP}$ and *m/z* 504 → 326 for dFd-CTP. Due to the lack of
646 commercially available standards of $^{13}\text{C}_3\text{-Ara-CTP}$ and dFd-CTP, relative quantification was
647 performed by comparing the peak area ratios (analyte/IS) of the differently treated samples.

648

649 **Production of lentiviral expression vectors and VLPs.** Lentiviral vectors expressing
650 SAMHD1-WT or SAMHD1-D311A were generated by co-transfection of packaging vector
651 pPAX2, either pHRSAMHD1-WT or pHRSAMHD1-D311A and a plasmid encoding VSV-
652 G. VLPs, carrying either Vpx or Vpr from SIVmac251, were produced by co-transfection of
653 293T cells with pSIV3+ *gag pol* expression plasmids and a plasmid encoding VSV-G. The
654 SAMHD1 degradation capacity of Vpx-VLPs was determined in THP-1 cells 24 h post
655 transduction by intracellular SAMHD1 staining.

656

657 **Manipulation of intracellular SAMHD1 levels.** For shRNA-mediated silencing of
658 *SAMHD1*, OCI-AML3 cells were transduced by spinoculation with VSV-G pseudotyped
659 lentiviral vectors carrying either pLKO.1-puro-control-shRNA or pLKO.1-puro-SAMHD1-
660 shRNA#1-3. On day 10 after transduction, successfully transduced cells were selected with
661 puromycin (P8833, Sigma-Aldrich) (7.5 µg/ml). SAMHD1 levels were monitored by
662 intracellular SAMHD1 staining and Western blotting. For siRNA-mediated silencing, AML
663 cells (1.2×10^6) were transfected with 2.5 µM ON-TARGET plus human *SAMHD1* siRNA
664 SMART-pool (L-013950-01-0050, Dharmacon) in resuspension electroporation buffer R
665 (Invitrogen) using the Neon transfection system (Invitrogen). Additionally, ON-TARGET
666 plus Non-targeting Pool (D-001810-10-50, Dharmacon) was transfected in parallel.
667 Electroporation was performed using one 20 msec pulse of 1700 V and analyzed 48 h post-
668 transfection via Western blotting and cell viability assay. The following siRNA duplexes were
669 used: non-targeting (UGGUUUACAUGUCGACUAA; UGGUUUUACAUGUUGUGUGA;
670 UGGUUUUACAUGUUUCUGA; UGGUUUUACAUGUUUUCCUA),
671 *SAMHD1* (GACAAUGAGUUGCGUAUUU; CAUGUUUGAUGGACGAAU;
672 AAGUAUUGCAGACGUGAA; UUAGUUUAUCCAGCGAUU).

673 HEL cells were transduced by spinoculation with VSV-G pseudotyped lentiviral vectors
674 carrying either SAMHD1-WT or the D311A mutant. Expression of SAMHD1 was monitored
675 by intracellular SAMHD1 staining and Western blotting. AML cell lines and primary AML
676 blasts were spinoculated with VSV-G pseudotyped VLPs carrying either Vpx or Vpr.

677

678 **HPLC assays for hydrolysis.** To investigate whether or not Ara-CTP or dFd-CTP are
679 hydrolyzed by SAMHD1, HPLC assays were performed as described previously³⁹. The
680 reaction mixtures (50 µl) contained 50 mM Tris-HCl (pH 7.5), 10 mM MgCl₂, 100 mM NaCl,
681 1 mM DTT, 1 mM Ara-CTP or dFdCTP, 0.2 mM activator (dGTP), and SAMHD1 (4 µM). In
682 some experiments, the SAMHD1 substrate TTP was used as positive control. Reaction
683 mixtures were incubated at 37°C and passed through 10K VWR Centrifugal Filters to quench
684 the reactions and remove the protein. Reaction products were analyzed by ion-pair reverse-
685 phase HPLC using a Varian Pursuit C18 column (150 × 4.6 mm) in a Varian ProStar HPLC
686 system with a photodiode array detector set at 260 nm. The mobile phase for separation of
687 nucleotides consisted of two eluants: 0.1 mM KH₂PO₄ (pH 6.0) with 8
688 mM tetrabutylammonium hydroxide and 0.1 mM KH₂PO₄ (pH 6.0) with 8
689 mM tetrabutylammonium hydroxide and 30 % methanol.

690

691 **Statistical analysis.** Statistical data analysis was performed using GraphPad Prism. Linear
692 regression and nonlinear fitting using one phase decay was used to assess correlation of
693 protein expression, mRNA levels, or IC₅₀ values (**Fig. 1, Supplementary Figs. 2,3,15,17**). R²
694 were used to assess the quality of the fit. Unpaired group comparisons were performed using
695 Student's *t*-test. In **Supplementary Fig. 11**, paired group comparisons were performed using
696 Student's *t*-test. F-test was used to assess significance of regression models (**Supplementary**

697 **Fig. 3).** Comparisons of multiple groups were performed using 1-way ANOVA. Statistical
698 data analysis of AML patient data was performed in R version 3.2.5
699 (R Core Team, 2016, <https://www.R-project.org/>), using Kaplan-Meier analysis and logrank
700 test for survival analysis.

701

702 **Data availability**

703 The Cancer Genome Atlas data (TCGA) can be retrieved using the RTCGA-Toolbox
704 R/BioConductor package, version 2.2.2. Plasmids are available upon request.

705

- 706
- 707 26. Keppler, O.T., *et al.* Susceptibility of rat-derived cells to replication by human
708 immunodeficiency virus type 1. *J Virol* **75**, 8063-8073 (2001).
- 709 27. Capes-Davis, A., *et al.* Match criteria for human cell line authentication: where do we
710 draw the line? *Int J Cancer* **132**, 2510-2519 (2013).
- 711 28. Wittmann, S., *et al.* Phosphorylation of murine SAMHD1 regulates its antiretroviral
712 activity. *Retrovirology* **12**, 103 (2015).
- 713 29. Vick, B., *et al.* An advanced preclinical mouse model for acute myeloid leukemia
714 using patients' cells of various genetic subgroups and in vivo bioluminescence
715 imaging. *PLoS One* **10**, e0120925 (2015).
- 716 30. Thomas, D., Herold, N., Keppler, O.T., Geisslinger, G. & Ferreiros, N. Quantitation of
717 endogenous nucleoside triphosphates and nucleosides in human cells by liquid
718 chromatography tandem mass spectrometry. *Anal Bioanal Chem* **407**, 3693-3704
719 (2015).
- 720 31. Kotchetkov, R., *et al.* Increased malignant behavior in neuroblastoma cells with
721 acquired multi-drug resistance does not depend on P-gp expression. *Int J Oncol* **27**,
722 1029-1037 (2005).
- 723 32. Michaelis, M., *et al.* Adaptation of cancer cells from different entities to the MDM2
724 inhibitor nutlin-3 results in the emergence of p53-mutated multi-drug-resistant cancer
725 cells. *Cell Death Dis* **2**, e243 (2011).
- 726 33. Michaelis, M., *et al.* Identification of flubendazole as potential anti-neuroblastoma
727 compound in a large cell line screen. *Sci Rep* **5**, 8202 (2015).
- 728 34. Riccardi, C. & Nicoletti, I. Analysis of apoptosis by propidium iodide staining and
729 flow cytometry. *Nat Protoc* **1**, 1458-1461 (2006).
- 730 35. Oellerich, T., *et al.* FLT3-ITD and TLR9 use Bruton tyrosine kinase to activate
731 distinct transcriptional programs mediating AML cell survival and proliferation. *Blood*
732 **125**, 1936-1947 (2015).
- 733 36. Samur, M.K. RTCGAToolbox: a new tool for exporting TCGA Firehose data. *PLoS*
734 *One* **9**, e106397 (2014).

- 735 37. Heuser, M., *et al.* MN1 overexpression induces acute myeloid leukemia in mice and
736 predicts ATRA resistance in patients with AML. *Blood* **110**, 1639-1647 (2007).
- 737 38. Goffinet, C., Schmidt, S., Kern, C., Oberbremer, L. & Keppler, O.T. Endogenous
738 CD317/Tetherin limits replication of HIV-1 and murine leukemia virus in rodent cells
739 and is resistant to antagonists from primate viruses. *J Virol* **84**, 11374-11384 (2010).
- 740 39. Beloglazova, N., *et al.* Nuclease activity of the human SAMHD1 protein implicated in
741 the Aicardi-Goutieres syndrome and HIV-1 restriction. *J Biol Chem* **288**, 8101-8110
742 (2013)
- 743

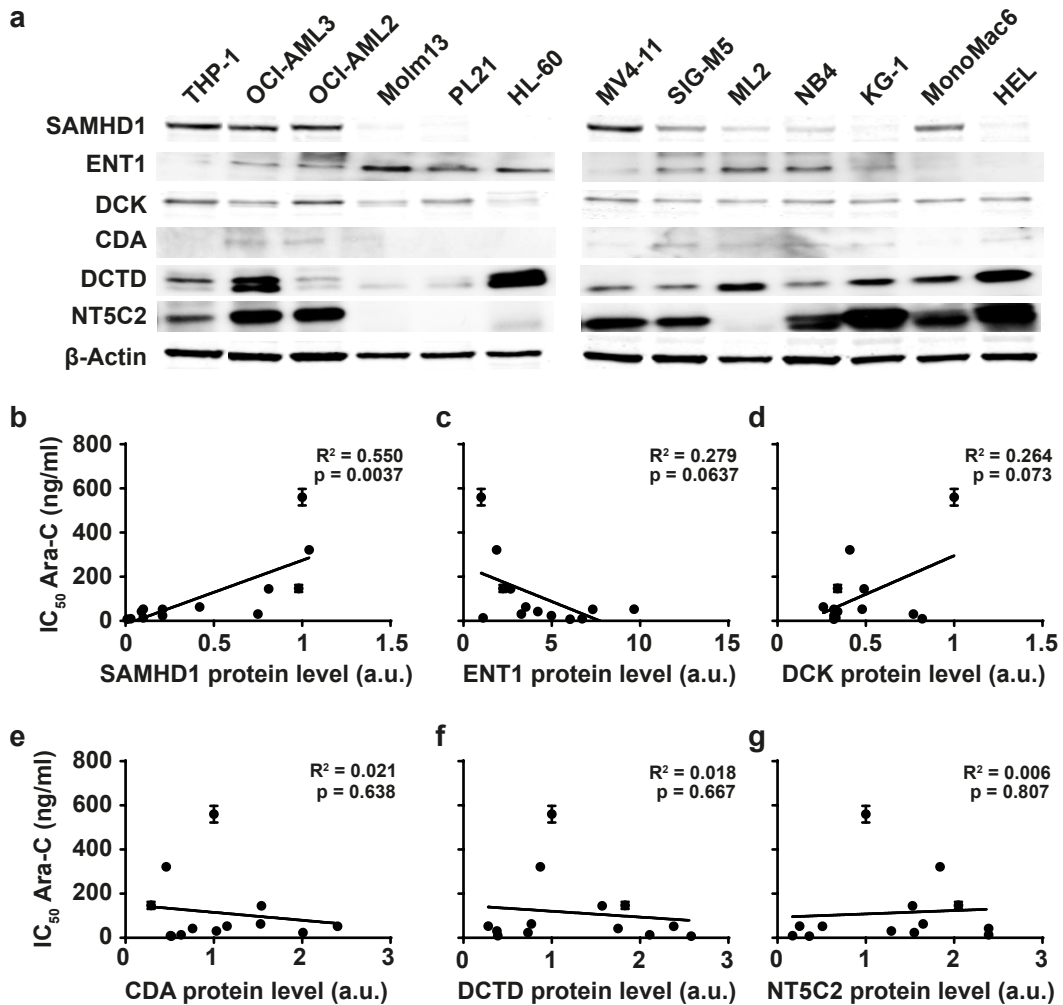
744 **Editorial summary**

745 The therapeutic response of acute myeloid leukemia to the nucleoside analog Ara-C is
746 regulated by SAMHD1, an enzyme which is differentially expressed in this cancer and which
747 hydrolyzes the active metabolite Ara-CTP.

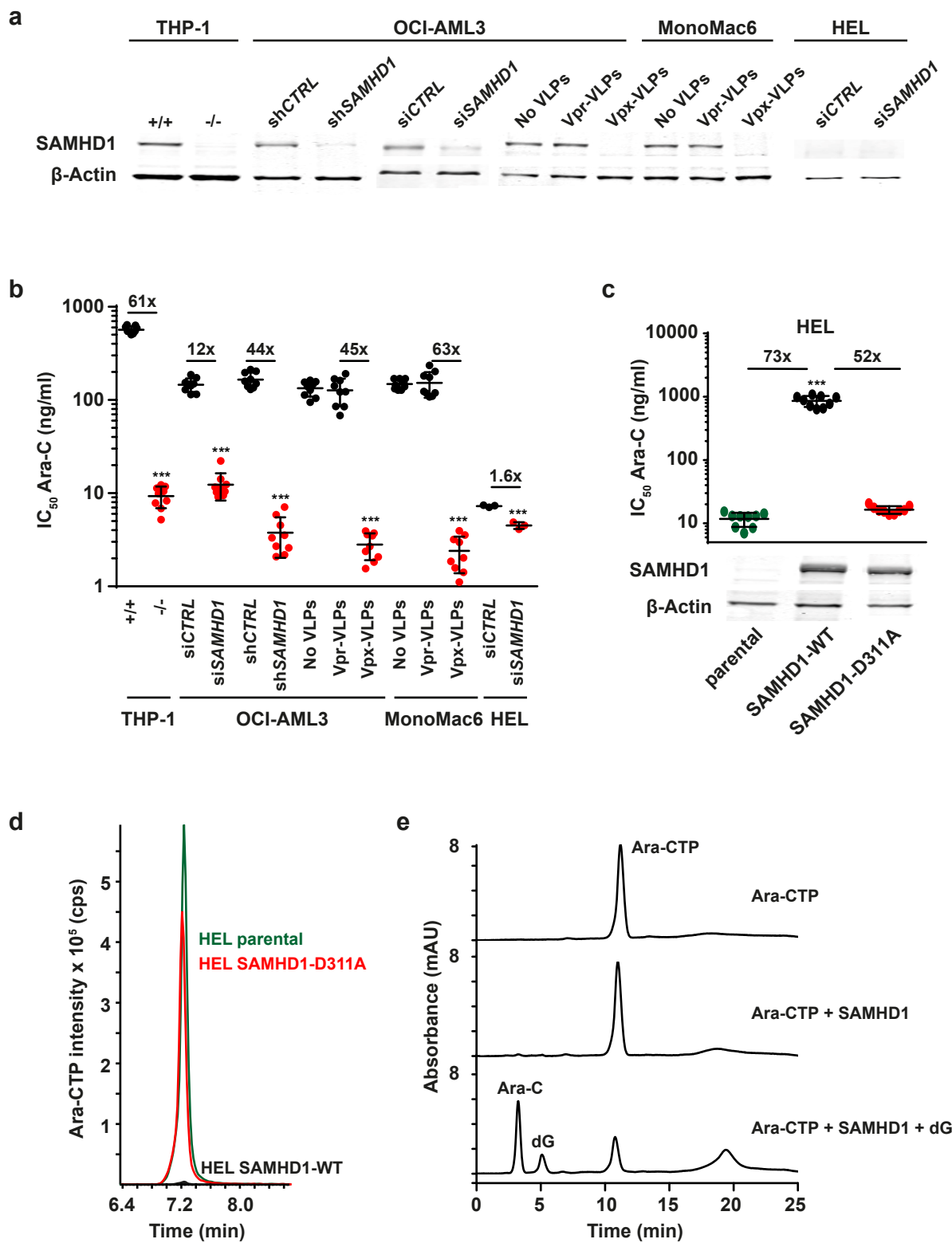
748

749

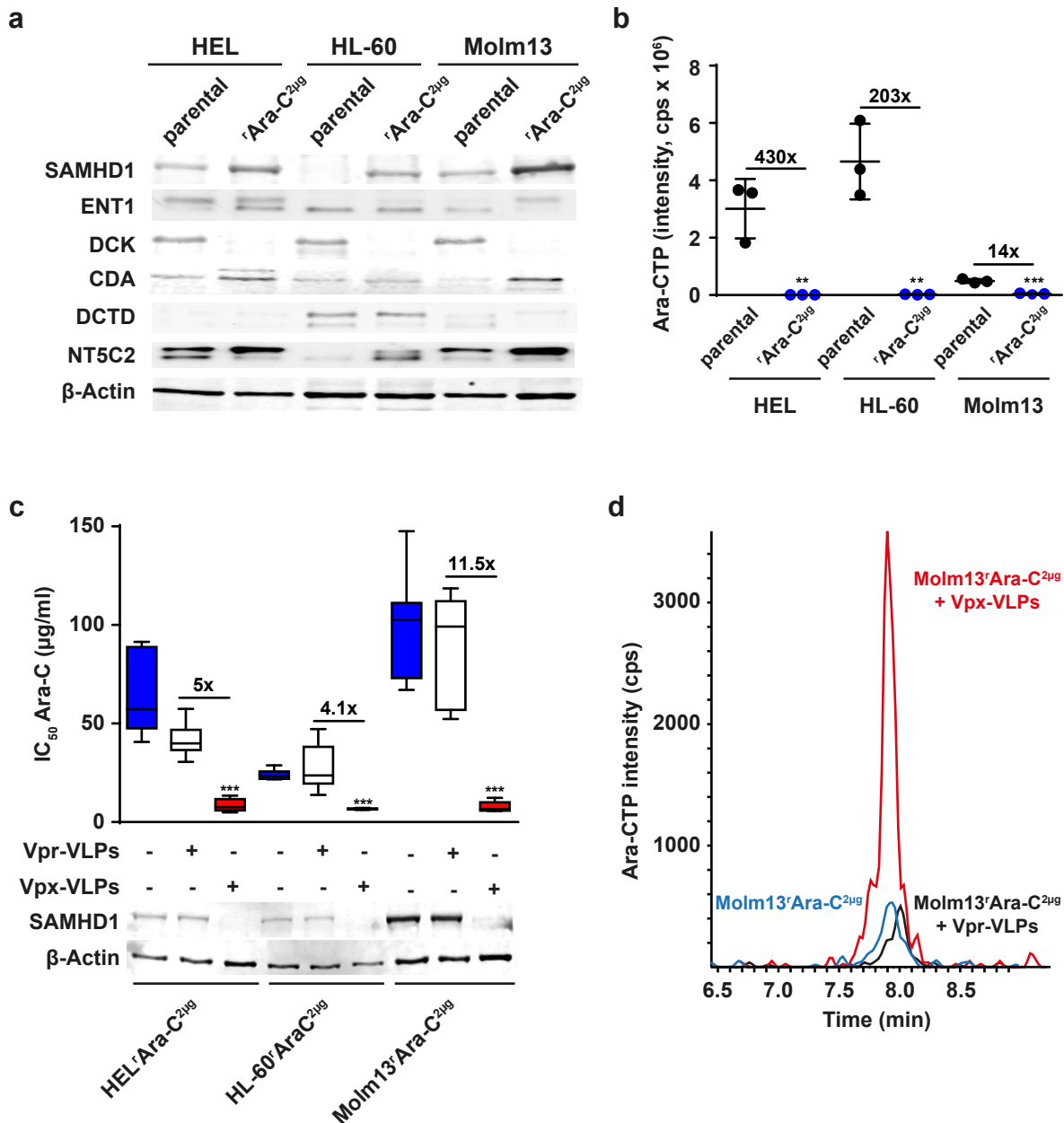
Schneider *et al.*, Figure 1



Schneider et al., Figure 2



Schneider et al., Figure 3



Schneider et al., Figure 4

